

Anomalous Quantum Reflection of Bose-Einstein Condensates from a Silicon Surface: The Role of Dynamical Excitations

R. G. Scott,¹ A. M. Martin,² T. M. Fromhold,¹ and F. W. Sheard¹

¹*School of Physics and Astronomy, University of Nottingham, Nottingham NG7 2RD, United Kingdom*

²*School of Physics, University of Melbourne, Parkville, Victoria 3010, Australia*

(Received 14 December 2004; published 11 August 2005)

We investigate the effect of interatomic interactions on the quantum-mechanical reflection of Bose-Einstein condensates from regions of rapid potential variation. The reflection process depends critically on the density and incident velocity of the condensate. For low densities and high velocities, the atom cloud has almost the same form before and after reflection. Conversely, at high densities and low velocities, the reflection process generates solitons and vortex rings that fragment the condensate. We show that this fragmentation can explain the anomalously low reflection probabilities recently measured for low-velocity condensates incident on a silicon surface.

DOI: [10.1103/PhysRevLett.95.073201](https://doi.org/10.1103/PhysRevLett.95.073201)

PACS numbers: 34.50.Dy, 03.75.Kk, 03.75.Lm

There is great current interest in using condensed matter systems to provide new tools for manipulating ultracold atoms, for example, micron-scale current-carrying wires on a semiconductor surface [1]. Understanding and controlling interactions between the atoms and the surface is crucial for the development of these “atom chips.” Recent experimental studies of Na-atom Bose-Einstein condensates (BECs) bouncing off a Si surface provide a powerful probe of such interactions [2]. When the approach velocity, v_x , is low, the rapid variation of the surface potential causes quantum-mechanical reflection (QR) of the atom cloud. Although quantum-mechanical calculations predict that the reflection probability for a *single* atom will increase monotonically as v_x decreases [2,3], the measured reflection probability for the BEC *decreases* with decreasing v_x below ~ 2 mm s⁻¹: an interesting observation that is not yet understood [2].

In this Letter, we show that interatomic interactions can have a pronounced effect on the QR of BECs from Si surfaces, consistent with the anomalously low reflection probabilities observed in experiment [2]. Our results demonstrate that the underlying physics is a *generic* feature of the reflection of BECs from regions of rapid potential variation, attractive or repulsive. As the BEC approaches the surface, its density profile is modulated by the standing wave formed by superposition of incident and reflected matter waves. Because of the interatomic interactions in a BEC, this modulation can have a dramatic effect on the reflection process. In particular, for high density BECs and low incident velocities, it triggers the formation of dynamical excitations (solitons and vortex rings) that fragment the atom cloud. Our analysis shows that although this fragmentation has no *intrinsic* effect on the reflection probability, it disperses the atoms and can therefore produce an *apparent* reduction in the reflection probability at low velocities, as observed in experiment [2]. Our calculations enable us to identify regimes in which the fragmentation of the atom cloud that accompanies low-speed QR should be

either strongly enhanced or suppressed, and thereby propose new experiments to test our interpretation of the reflection process.

We consider BECs containing N ²³Na atoms in a cylindrically symmetrical harmonic trap. First we take parameters from recent experiments [2]: $N = 3 \times 10^5$ and longitudinal (radial) trap frequencies $\omega_x(\omega_r) = 2\pi \times 3.3(2\pi \times 4.5)$ rad s⁻¹, which produce an atom cloud of equilibrium peak density $n_0 = 2.2 \times 10^{12}$ cm⁻³. At time $t = 0$ ms, we suddenly displace the harmonic trap by a distance Δx along the x direction [2], and hence accelerate the BEC towards a region of rapid potential energy variation at $x = \Delta x$. We consider three different potential profiles: potential I [$V_I(x)$, solid curve in Fig. 1(a)] is a sharp potential step of height $V_s = 10^{-30}$ J; potential II [$V_{II}(x)$, solid curve in Fig. 1(b)] is an abrupt potential drop of depth V_s ; potential III [$V_{III}(x)$, solid curve in Fig. 1(c)] is a model of the Si surface, whose form is specified later. The model potentials I and II enable us to identify the key physical processes that occur when a BEC undergoes reflection, and thereby develop the understanding required to interpret experimental studies of BECs reflecting from the more complicated Si surface potential. Following the trap displacement, the total potential energy of each Na atom (mass m) in the BEC is $V_T(x, r) = V_{\text{step}}(x) + \frac{1}{2}m[\omega_x^2(x - \Delta x)^2 + \omega_r^2 r^2]$, where r is the radial coordinate and $V_{\text{step}}(x)$ is $V_I(x)$, $V_{II}(x)$, or $V_{III}(x)$.

We determine the dynamics of the BEC in three dimensions by using the Crank-Nicolson [4] method to solve the time-dependent Gross-Pitaevskii equation [5,6]

$$i\hbar \frac{\partial \Psi}{\partial t} = \left[-\frac{\hbar^2}{2m} \nabla^2 + V_T(x, r) + \frac{4\pi\hbar^2 a}{m} |\Psi|^2 \right] \Psi \quad (1)$$

where ∇^2 is the Laplacian in cylindrical coordinates, $a = 2.9$ nm is the s -wave scattering length, and $\Psi(x, r, t)$ is the axially symmetrical condensate wave function at time t , normalized such that $|\Psi|^2$ is the number of atoms per unit

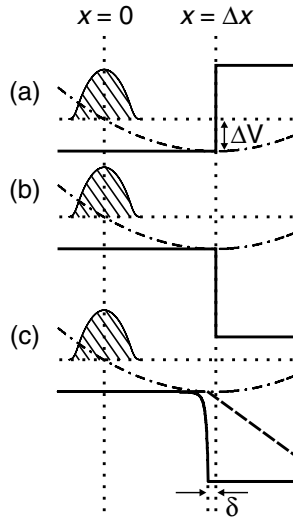


FIG. 1. Solid curves: schematic representations of $V_I(x)$ (a), $V_{II}(x)$ (b), and $V_{III}(x)$ (c). Dot-dashed curves: the potential energy of the harmonic trap, shown as a function of x , immediately after the trap displacement. Shaded areas in (a)–(c) represent the initial atom density profile $|\Psi(x, 0, 0)|^2$. Dashed line in (c) shows the imaginary potential used to model the adsorption of Na atoms on the Si surface.

volume. The equilibrium density profile of the BEC in the harmonic trap is shown in Fig. 2(a).

We now explore the dynamics of the BEC in potential I. When the trap is displaced at $t = 0$ ms, the initial potential energy of the BEC is increased by $\Delta V \approx \frac{1}{2} m \omega_x^2 \Delta x^2$, as shown in Fig. 1(a), causing the atoms to be incident on the potential step with a velocity $v_x \approx \omega_x \Delta x$. For the displacements considered here, $\Delta V \ll V_s$. Hence, in a classical picture, we expect the BEC to be completely reflected by the step. Figure 2 shows images of the BEC undergoing reflection from potential I after a trap displacement of $60 \mu\text{m}$, for which $v_x \approx 1.2 \text{ mm s}^{-1}$. At $t = 90$ ms [Fig. 2(b)], approximately half the atoms have reached the barrier, and a standing wave has formed as a result of the superposition of the incident and reflected waves, causing periodic modulations in the density profile. Because of the interatomic interactions, the high density at the peaks of the standing wave causes atoms to be pushed out from the axis of cylindrical symmetry (the x axis), thus transferring momentum into the transverse direction. These atoms appear as the arrowed jetlike “lobes” at the top and bottom of Fig. 2(b). The lobes ride up the walls of the harmonic trap and are then reflected back towards the x axis. This causes a cylindrically symmetrical soliton to form, which appears as the two white stripes (arrowed) in Fig. 2(c). The soliton then decays via the snake instability [7] into two vortex rings centered on $r = 0$, which appear as pairs of density nodes within the dashed box in Fig. 2(d). The phase of the BEC wave function within the dashed box in Fig. 2(d) is shown to the right of the density profile. The figure reveals a 2π phase change around each density node, indicating quantized circulation.

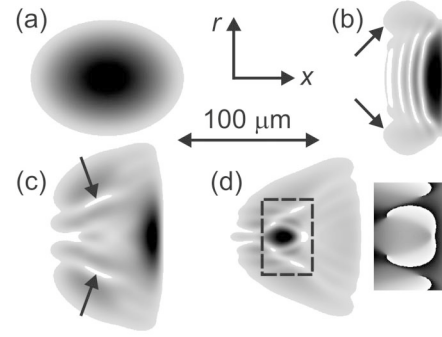


FIG. 2. Gray-scale plots of atom density (black = high) in the x - r plane (axes inset) for a BEC with $n_0 = 2.2 \times 10^{12} \text{ cm}^{-3}$, $\omega_x(\omega_r) = 2\pi \times 3.3(2\pi \times 4.5) \text{ rad s}^{-1}$ and $v_x \approx 1.2 \text{ mm s}^{-1}$, reflecting from potential I, shown at $t = 0$ ms (a), 90 ms (b), 122 ms (c), and 143 ms (d). The phase of the BEC wave function within the dashed box in (d) is shown in the gray-scale plot (white = 0, black = 2π) to the right of the density profile. Horizontal bar shows scale.

At the end of the oscillation, the atom cloud still contains vortex rings, and has a fragmented appearance [Fig. 3(a)]. Similar dynamics have been observed for two-dimensional BECs reflecting from a circular hard wall [8].

For disruption to occur, the time taken for lobes to form, $t_L \approx l_r/v_s$, where l_r is the BEC’s radial width and $v_s \approx \sqrt{\hbar^2 n_0 a / \pi m^2}$ is the average speed of sound [9], must be less than the reflection time $t_R \approx l_x/v_x$, where l_x is the BEC’s longitudinal width. We therefore estimate that reflection will *not* significantly disrupt the BEC when

$$v_x \geq v_s(l_x/l_r), \quad (2)$$

or, equivalently, when $\Delta x \geq (v_s l_x)/(l_r \omega_x)$. Our numerical simulations confirm this [10]: for a large $v_x \approx 2.1 \text{ mm s}^{-1}$ ($\Delta x = 100 \mu\text{m}$), the reflected atom cloud at $t = 150$ ms [Fig. 3(b)] contains no excitations and has a smooth density

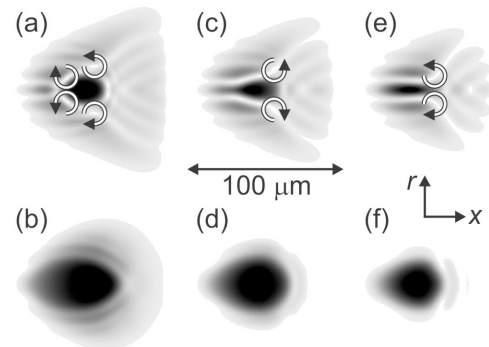


FIG. 3. Gray-scale plots of atom density (black = high) in the x - r plane (axes inset) for a BEC with $n_0 = 2.2 \times 10^{12} \text{ cm}^{-3}$, $\omega_x(\omega_r) = 2\pi \times 3.3(2\pi \times 4.5) \text{ rad s}^{-1}$, and $v_x \approx 1.2 \text{ mm s}^{-1}$ (a), 2.1 mm s^{-1} (b), reflecting from potential I, shown at $t = 150$ ms. (c),(d) Same as (a),(b), but for potential II. (e),(f) Same as (a),(b), but for potential III. Horizontal bar shows scale. Arrows in (a),(c), and (e) indicate the direction of quantized circulation around vortex cores.

profile, similar to the original BEC ground state [Fig. 2(a)]. Similar behavior has been reported for BECs on Bragg reflection in optical lattices [6,11–13].

We now consider QR of a BEC from the abrupt potential drop (potential II) shown in Fig. 1(b). The reflected atom clouds at $t = 150$ ms for $v_x \approx 1.2$ and 2.1 mm s $^{-1}$ are shown in Figs. 3(c) and 3(d), respectively. They are remarkably similar to the equivalent images for potential I [Figs. 3(a) and 3(b)], except that they are slightly smaller because fewer atoms are reflected. When $v_x \approx 1.2$ mm s $^{-1}$, the reflected atom cloud has a fragmented appearance and contains a vortex ring, enclosed by the arrows in Fig. 3(c). By contrast, when $v_x \approx 2.1$ mm s $^{-1}$ the BEC contains no excitations and has a smooth density profile [Fig. 3(d)]. This is because, as for potential I, when $v_x \approx 2.1$ mm s $^{-1}$ the reflection process is too fast for side lobes to form in response to the standing wave.

Having studied two simple potential steps, we now investigate QR from a Si surface [2] at $x = \Delta x$, which we model by potential III [$V_{\text{III}}(x)$, solid curve in Fig. 1(c)]. Potential III is based on the Casimir-Polder potential $V_{\text{CP}}(x') = -C_4/x'^3(x' + 3\lambda_a/2\pi^2)$, where $C_4 = 9.1 \times 10^{-56}$ J m 4 , $\lambda_a = 590$ nm is the effective atomic transition wavelength [14], and $x' = x - \Delta x$ is the distance from the surface. For $x < \Delta x - \delta$, where $\delta = 0.15$ μm is a small offset from the surface [Fig. 1(c)], we set $V_{\text{III}}(x) = V_{\text{CP}}(x')$. However, since $V_{\text{CP}} \rightarrow -\infty$ as $x \rightarrow \Delta x$, for $x \geq \Delta x - \delta$ we set $V_{\text{III}}(x) = V_{\text{CP}}(\delta) - i(x - \Delta x + \delta)V_{\text{im}}$, where $V_{\text{im}} = 1.6 \times 10^{-26}$ J m $^{-1}$. No atoms are reflected when $x \geq \Delta x - \delta$ because the real part of $V_{\text{III}}(x)$ is constant. The imaginary part of $V_{\text{III}}(x)$ [dashed curve in Fig. 1(c)] models adsorption of Na atoms by the Si surface [15]. We expect that the BEC will undergo QR when $|d\lambda/dx| \geq 1$ [3], where λ is the local de Broglie wavelength. For $v_x = 1$ mm s $^{-1}$, most atoms reflect ~ 1 μm from the surface, where $|d\lambda/dx|$ is maximal [16].

Figures 3(e) and 3(f) show the reflected atom clouds at $t = 150$ ms for $v_x \approx 1.2$ and 2.1 mm s $^{-1}$ respectively. Although they are smaller than the corresponding images for potentials I and II because fewer atoms are reflected, the qualitative behavior of the BEC is the same. When $v_x \approx 1.2$ mm s $^{-1}$, the atom cloud is disrupted and contains a vortex ring [Fig. 3(e)], whereas for $v_x \approx 2.1$ mm s $^{-1}$ the BEC has a smooth density profile and contains no excitations [Fig. 3(f)]. This is consistent with the experiments of Pasquini *et al.* [2], who observed “excited and sometimes fragmented” atom clouds following the QR of BECs incident on a Si surface at low v_x .

To quantify how the QR process depends on v_x , and to relate our simulations to experiment [2], we made numerical calculations of the probability, R , that each atom in the BEC will quantum reflect from the Si surface potential. The solid curves in Fig. 4 show R versus v_x calculated for atom clouds with (squares) and without (crosses) interatomic interactions. In each case, R increases with decreasing v_x . Similar behavior was reported for *single* atoms in Refs. [2,3,17].

A key feature of Fig. 4 is that the $R(v_x)$ curves calculated with and without interatomic interactions are nearly identical, indicating that the interactions have little *intrinsic* effect on R [18]. Consequently, interatomic interactions do not *immediately* explain why experimentally measured R values *decrease* with decreasing $v_x \lesssim 2$ mm s $^{-1}$ [2]. However, a possible explanation of this anomalous behavior does emerge when we consider how the interactions affect the structure of the BEC at low v_x . In the absence of interactions, QR does *not* change the form of the atom cloud. By contrast, interactions cause disruption and fragmentation of the atom cloud when $v_x \lesssim 2$ mm s $^{-1}$ ($\Delta x \lesssim 80$ μm): precisely the regime where anomalously low R values are observed in experiment [2]. Severe disruption of the cloud can make detection of atoms difficult in low-density regions of the BEC [19], facilitate thermal excitation, or even eject atoms from the trap [20], thus accounting for the anomalously low R values observed in experiment. To simulate the effect of such losses, we recalculated R omitting the contribution from atoms in low-density regions of the BEC for which $|\Psi|^2 \leq n_c$, where n_c is a threshold below which detection of atoms can be difficult [19]. The dotted curve with circles in Fig. 4 shows $R(v_x)$ calculated for $n_c = 0.25 n_0$. In this case, R dips below the equivalent single-atom result for $v_x < 2$ mm s $^{-1}$ as in experiment [2], and then decreases with decreasing $v_x < v_p \approx 1.5$ mm s $^{-1}$, in the regime where severe fragmentation of the atom cloud produces large areas of low density [21].

To explore the parameter space, we repeated our calculations for BECs in the same harmonic trap as before, but

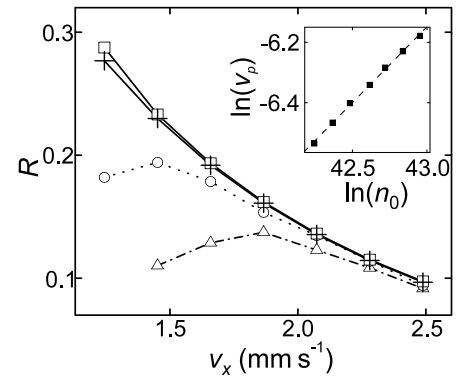


FIG. 4. Solid curves: $R(v_x)$ for potential III, calculated from the entire reflected atom cloud with (squares) and without (crosses) interatomic interactions. Dotted curve with circles: $R(v_x)$ calculated with interatomic interactions, but omitting regions of the atom cloud where $|\Psi|^2 \leq 0.25 n_0$. For the solid and dotted curves, $n_0 = 2.2 \times 10^{12}$ cm $^{-3}$ and $\omega_x(\omega_r) = 2\pi \times 3.3(2\pi \times 4.5)$ rad s $^{-1}$. Dot-dashed curve with triangles: as dotted curve with circles, but for a BEC with $n_0 = 3.6 \times 10^{12}$ cm $^{-3}$. Inset: data points (squares) show $\ln(v_p)$ vs $\ln(n_0)$, where v_p is the position of the peak in $R(v_x)$ curves calculated omitting regions where $|\Psi|^2 \leq 0.25 n_0$, and dashed line is least squares fit.

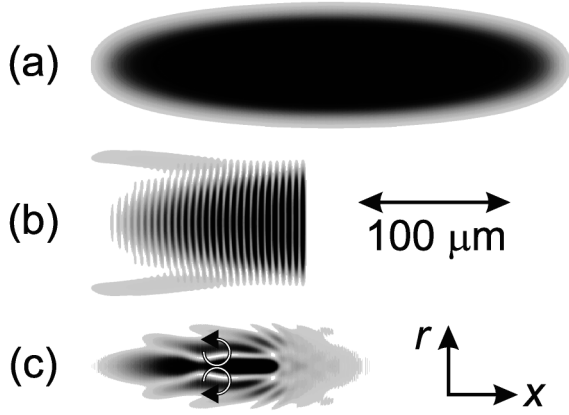


FIG. 5. Gray-scale plots of atom density (black = high) in the x - r plane (axes inset) for a BEC with $n_0 = 2.2 \times 10^{12} \text{ cm}^{-3}$, $\omega_x(\omega_r) = 2\pi(2\pi \times 4.5) \text{ rad s}^{-1}$, and $v_x \approx 2.1 \text{ mm s}^{-1}$, reflecting from potential III, shown at $t = 0 \text{ ms}$ (a), 270 ms (b), and 460 ms (c). Horizontal bar shows scale. Arrows in (c) enclose a vortex ring.

with different values of N and n_0 . When we increase N to 10^6 ($n_0 = 3.6 \times 10^{12} \text{ cm}^{-3}$), the peak in our calculated $R(v_x)$ curve (dot-dashed in Fig. 4) occurs at a higher v_p of 1.9 mm s^{-1} (corresponding to $\Delta x = 90 \mu\text{m}$). Simulations for BECs with a range of N reveal that a plot of $\ln(v_p)$ versus $\ln(n_0)$ (Fig. 4 inset) is linear, with a gradient of 0.5 ± 0.01 . This is because the peak in $R(v_x)$ coincides with the onset of disruption of the atom cloud so that, from inequality (2), $v_p \propto \sqrt{n_0}(l_x/l_r) \propto \sqrt{n_0}$, as (l_x/l_r) is independent of N and n_0 for the trap considered above. According to this analysis, for given n_0 , v_p will be higher for a more cigar-shaped BEC. To confirm this, we investigated QR for an elongated atom cloud [Fig. 5(a)] formed by reducing ω_x to $2\pi \text{ rad s}^{-1}$ and changing N to 9.8×10^5 to maintain the original value of $n_0 = 2.2 \times 10^{12} \text{ cm}^{-3}$. For $v_x \approx 2.1 \text{ mm s}^{-1}$ ($\Delta x = 330 \mu\text{m}$), large side lobes form during QR [Fig. 5(b)], leading to fragmentation of the atom cloud and production of a vortex ring [Fig. 5(c)] [22]. By contrast, for the same values of n_0 and v_x , the more spherical BEC shown in Fig. 2(a) is not disrupted by QR [Fig. 3(f)].

In summary, we have investigated the reflection of BECs from three abrupt potential steps, and shown that the dynamics are qualitatively the same in each case. For high v_x , reflection occurs cleanly, causing almost no change in the atom density profile. But at low v_x , the standing wave formed from the superposition of the incident and reflected waves generates dynamical excitations that disrupt the atom cloud. This disruption could explain the anomalously low R values recently measured for BECs incident on a Si surface at low velocity. Fragmentation of the atom cloud is particularly dramatic for dense slow-moving cigar-shaped BECs, and further experiments in this regime would test our interpretation of the reflection process. Conversely, for low-density BECs, which are not

significantly disrupted by QR, the observed values of R should continue to increase with decreasing v_x , even when v_x is small. In this regime, QR near a Si surface should provide an effective means of containing BECs and decoupling them from the surface.

We thank T. Pasquini and O. Morsch for helpful discussions. This work is funded by EPSRC UK and ARC.

-
- [1] W. Hänsel, P. Hommelhoff, T. Hänsch, and J. Reichel, *Nature (London)* **413**, 498 (2001).
 - [2] T. Pasquini *et al.*, *Phys. Rev. Lett.* **93**, 223201 (2004).
 - [3] F. Shimizu, *Phys. Rev. Lett.* **86**, 987 (2001).
 - [4] D.-I. Choi and Q. Niu, *Phys. Rev. Lett.* **82**, 2022 (1999).
 - [5] R. G. Scott *et al.*, *Phys. Rev. Lett.* **90**, 110404 (2003).
 - [6] R. G. Scott *et al.*, *Phys. Rev. A* **69**, 033605 (2004).
 - [7] Z. Dutton, M. Budde, C. Slowe, and L. V. Hau, *Science* **293**, 663 (2001).
 - [8] J. Ruostekoski, B. Kneer, W. Schleich, and G. Rempe, *Phys. Rev. A* **63**, 043613 (2001).
 - [9] C. Pethick and H. Smith, *Bose-Einstein Condensation in Dilute Gases* (Cambridge University Press, Cambridge, England, 2002).
 - [10] Inequality (2) captures the essential physics of the reflection process and gives a qualitative estimate of the threshold v_x required to suppress disruption of the BEC.
 - [11] M. Cristiani *et al.*, *Opt. Express* **12**, 4 (2004).
 - [12] Y. Zheng, M. Kostrun, and J. Javanainen, *Phys. Rev. Lett.* **93**, 230401 (2004).
 - [13] During Bragg reflection of a BEC in an optical lattice, side lobes do not form because the standing wave extends across the entire atom cloud. In this case, other mechanisms can trigger disruption of the atom cloud (see, for example, [4–6,11,20] and references therein).
 - [14] H. Casimir and D. Polder, *Phys. Rev.* **73**, 360 (1948).
 - [15] We assume that atoms which do not undergo QR are either adsorbed by the Si or scatter inelastically [2].
 - [16] $|d\lambda/dx|$ becomes <1 close to the surface (for $x' \leq 0.04 \mu\text{m}$ when $v_x = 1 \text{ mm s}^{-1}$). Choosing $\delta = 0.15 \mu\text{m}$ ensures that $V_{\text{III}}(x)$ incorporates most of the reflecting region, while avoiding regions where the Casimir-Polder potential varies too rapidly with x' to allow accurate discretization of the wave function.
 - [17] H. Friedrich, G. Jacoby, and C. Meister, *Phys. Rev. A* **65**, 032902 (2002).
 - [18] For potential II, R can be determined analytically in the absence of interatomic interactions by imposing the usual wave function matching conditions at $x = \Delta x$. The R values obtained in this way for a single atom are within $\sim 5\%$ of those determined for a BEC from our numerical solution of Eq. (1): indicating that interatomic interactions have little effect on the R values for potential II (as shown for potential III in Fig. 4).
 - [19] O. Morsch (private communication).
 - [20] L. Fallani *et al.*, *Phys. Rev. Lett.* **93**, 140406 (2004).
 - [21] We see qualitatively similar behavior for all $n_c \geq 0.1n_0$.
 - [22] The reflected atom cloud [Fig. 5(c)] is much smaller than the incident cloud [Fig. 5(a)] because R is only 0.14.